Field Data Analysis for a Range-Based Local Airport Monitor for WAAS

Jiwon Seo, Jason Rife, Sam Pullen, Todd Walter, and Per Enge, *Stanford University*

ABSTRACT

The Local Airport Monitor (LAM) concept has been proposed as an inexpensive and rapidly deployable implementation of LAAS. The LAM combines WAAS corrections with local monitoring to provide an error bound tight enough to enable Category I precision approach and landing. Two different strategies for LAM have been proposed–a range-based method and a position-domain method [1,2]. Both methods monitor WAAS by computing a discrepancy between WAAS corrected pseudoranges and locally measured pseudoranges. The discrepancy impacts the navigation error bound, and accordingly the integrity, continuity, and availability of the method.

This paper analyzes field data in order to validate one of the proposed LAM implementations, the range-based method. The discrepancy statistic is computed for nine nominal days at Atlantic City. These data are exploited to validate performance simulations for LAM and to aid in selecting variable LAM parameters.

Specifically, this study focuses on four aspects of the data which impact LAM operations. First, the distribution of the discrepancy statistic is considered. This investigation verifies the theoretical distribution model used in previous LAM availability studies. Second, time correlation of the discrepancy signal is considered. Data analysis shows that low-frequency components of the discrepancy signal, which persist for about 1000 seconds or more, dominate the discrepancy model and strongly impact system continuity, which is computed over an approach window of only 150 seconds. Third, the combined impact of discrepancies for all satellites in view is analyzed in the position domain. This position-domain analysis validates LAM performance and enables selection of variable LAM parameters. Fourth, biases in the position-domain discrepancy statistic are considered. These biases, which are observed to vary for each 24-hour data set, may result in an availability and continuity penalty not considered in previous research. Together, these effects indicate the need for refinement of LAM performance simulations, but otherwise support the feasibility of the LAM concept.

INTRODUCTION

The Local Airport Monitor (LAM) concept was proposed by the Federal Aviation Administration (FAA) to accelerate deployment of Category I (CAT I) Local Area Augmentation System (LAAS). Difficult problems including ionosphere gradients and signal deformation have arisen during development of LAAS. These hazards have made LAAS certification increasingly complex and expensive. By contrast, the Wide Area Augmentation System (WAAS) is already in operation. Although today's WAAS cannot yet meet CAT I integrity standards, its accuracy, which is better than 2 m (95%), is sufficient to support CAT I approach operations under nominal conditions.

The basic idea of LAM is to implement additional WAAS monitoring at an airport to detect off-nominal system behavior. This monitoring enables the LAM to rebroadcast WAAS corrections with a tightened error bound, based on local monitoring. The LAM requires no changes to existing hardware, because WAAS corrections are broadcast to LAAS-equipped aircraft in the standard LAAS VHF Data Broadcast (VDB) format. Figure 1 conceptually shows LAM operation for CAT I precision approach.

The LAM could be significantly cheaper to install than conventional LAAS, because LAM will require fewer certified components. The LAM exploits already certified WAAS monitors, so the receiver hardware and software of the ground station would be much simpler than LAAS. However, LAM may not achieve the same CAT I availability as conventional LAAS, even though it achieves full CAT I integrity. Since LAM is designed for CAT I service only, LAAS is required for CAT II/III service in the future. Therefore, it is evident that the LAM is not a replacement for LAAS but a stepping-stone toward CAT II/III LAAS. More discussion about advantages and limitations of LAM is given in [3].

There are at least two proposed concepts for LAM implementation, which are a position-domain monitoring concept and a range-based concept. In the position-domain monitoring concept, which was suggested by

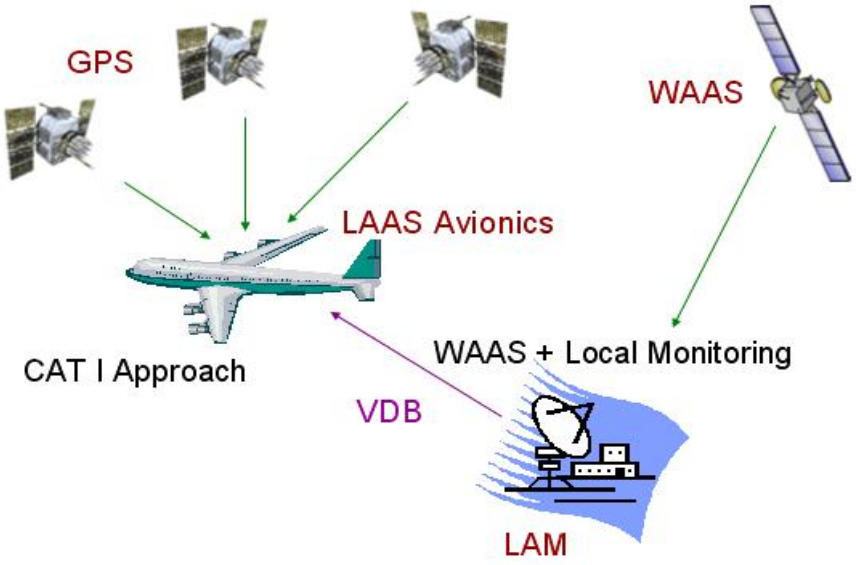

Figure 1. Local Airport Monitor Concept Diagram

MITRE [2], LAM computes a position solution applying WAAS corrections. If the difference of this position solution and the surveyed antenna location is below a certain threshold, the satellite set is declared to be usable for CAT I precision approach. On the other hand, the range-based LAM, which was proposed by Stanford [1], is more similar to conventional LAAS. The LAM ground station broadcasts the discrepancy between locally generated corrections and received WAAS corrections as a B-value. Then, a LAAS-equipped aircraft computes its own protection levels. Although both approaches are appropriate to implement LAM, this paper focuses on the range-based approach.

Since an aircraft calculates its protection levels in the range-based LAM relying on the broadcast discrepancy statistic, characteristics of the discrepancy signal need to be investigated to assess system performance parameters including availability and continuity. This paper evaluates statistics of the discrepancy signal using field data provided by the Federal Aviation Administration Technical Center (FAATC) to analyze the performance of the range-based LAM.

DISCREPANCY STATISTIC

In its role monitoring the WAAS broadcast, the key LAM measurement is the discrepancy between the WAAS pseudorange correction, W_i, and a locally derived pseudorange correction, L_i. The LAM evaluates this discrepancy, labeled δ_i in (1), for each of the N satellites in view. The discrepancy statistic is then incorporated into the error bound for the LAM.

$$\delta_i = L_i - W_i \tag{1}$$

For the range-based LAM, the discrepancy statistic is broadcast to the airborne user and inserted directly into the navigation error bound called the Vertical Protection Level (VPL). The equation for the LAM error bound, under fault-free conditions, is given as follows [1].

$$\mathrm{VPL}_{\mathrm{LAM}} = K_{bnd}\sqrt{\sum_{i=1}^{N} S_{v,i}^2 \sigma_{tot,i}^2} + \left|\sum_{i=1}^{N} S_{v,i}\delta_i\right| \tag{2}$$

$$\text{where } \sigma_{tot,i}^2 = \sigma_{L,i}^2 + \sigma_{air,i}^2 + \sigma_{iono,i}^2 + \sigma_{trop,i}^2$$

The second term of $\mathrm{VPL}_{\mathrm{LAM}}$ describes the discrepancy in the WAAS corrections, as measured by the LAM, and the first term describes the error in the LAM's local measurement.

All the parameters of the $\mathrm{VPL}_{\mathrm{LAM}}$ equation are well modeled, except for the discrepancy term, δ. Since the first term of $\mathrm{VPL}_{\mathrm{LAM}}$ resembles the nominal error term in the $\mathrm{VPL}_{\mathrm{H1}}$ equation for conventional LAAS, (3), appropriate models for the sigmas of the i^{th} ranging source have been well developed.

$$\mathrm{VPL}_{\mathrm{H1},j} = K_{md}\sqrt{\sum_{i=1}^{N} S_{v,i}^2 \sigma_{M,i}^2} + \left|\sum_{i=1}^{N} S_{v,i} B_{i,j}\right| \qquad (3)$$

$$\text{where } \sigma_{M,i}^2 = \frac{M_i}{M_i - 1}\sigma_{gnd,i}^2 + \sigma_{air,i}^2 + \sigma_{iono,i}^2 + \sigma_{trop,i}^2$$

Furthermore, once the integrity for the category of operation is allocated, the multiplier, K_{bnd} in (2) can be readily calculated.

Because the characteristics of the discrepancy term, δ, have not previously been evaluated in an experimental study, this paper seeks to evaluate these statistics in order to provide a more accurate means of assessing LAM performance characteristics including availability and continuity.

COMPUTING DISCREPANCY FROM DATA

In this paper, the statistics of the discrepancy, δ, are evaluated using field data provided by the Federal Aviation Administration Technical Center (FAATC). The FAATC data set described both WAAS corrections and local corrections for nine nominal days. The WAAS corrections were evaluated for Atlantic City, NJ, so that they corresponded to the local corrections, which were generated by the LAAS Test Prototype (LTP) installed at the Atlantic City airport.

In analyzing the discrepancy statistic for each satellite, the discrepancy equation, (1), was modified to account for antenna calibration effects. Position biases appeared in the data, in part because the WAAS and LAAS systems use different reference frames. A detailed explanation of the reference frame effect, and of other potential bias sources, is described in the later section titled *Frame Correction and Residual Bias*.

For the purposes of data analysis, the position-domain bias was removed for each day-long data set by computing the DC position bias, ΔP, and tilting it into the slant direction through the geometry factor, G_i. This bias-removal process transforms the standard discrepancy equation, (1), into the following form.

$$\delta_i = L_i - W_i - G_i \Delta P \qquad (4)$$

For real-time operations, the two forms of the discrepancy equation are identical, so long as the position-domain bias is zero.

PARAMETERIZING THE DISCREPANCY STATISTIC

Because discrepancy is nonstationary, its distribution changes in time. In order to capture these effects accurately, it is necessary to identify dependencies within the data set. Conceptually, discrepancy might be expected to depend both on satellite elevation and on quality metrics in the WAAS broadcast message. In practice, the discrepancy statistic depended most strongly on satellite elevation. This section details these dependency relationships and their impact on system availability performance.

Two WAAS error parameters were expected to correlate strongly with the standard deviation of the discrepancy statistic: the User Differential Range Error (UDRE) and the Grid Ionosphere Vertical Error (GIVE). The first of these parameters describes the impact of clock and ephemeris errors on WAAS, while the second describes the impact of the ionosphere error. Dependence on the GIVE parameter could not be evaluated with the available data set, which included only calm ionosphere days. However, dependence of the discrepancy statistic on the UDRE parameter was evaluated.

As illustrated in Figure 2, the data demonstrate that the correlation between User Differential Range Error Indicator (UDREI) and the discrepancy standard deviation is weak. The UDREI is a 4-bit discretization of the σ_{UDRE} parameter, which represents a bound on the standard deviation of the WAAS pseudorange correction error after applying fast and long-term corrections [4]. The figure indicates the lack of a trend for one day's data (November 5, 2004). The trend is no stronger on other days examined in the data set.

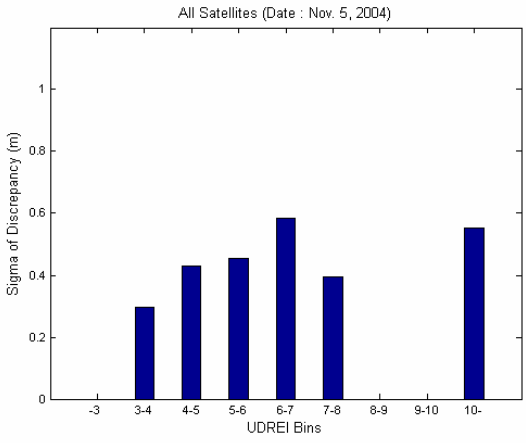

Figure 2. Correlation between UDREI and σ_δ

By contrast, the data show a strong dependency between the discrepancy standard deviation and satellite elevation. This relationship is illustrated in Figure 3 for the November 5 data.

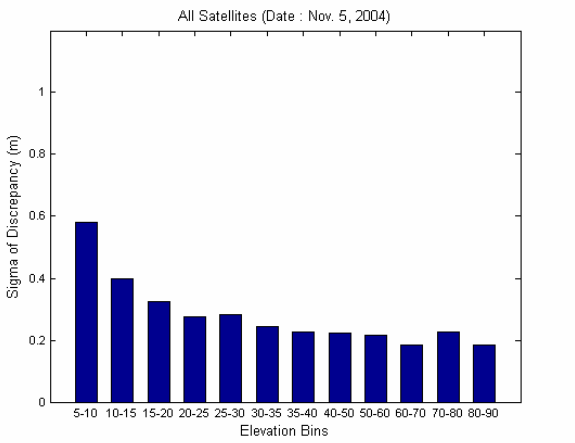

Figure 3. Dependency between Elevation and σ_δ

The other eight days' data show a consistent trend between the standard deviation of the discrepancy, σ_δ, and satellite elevation.

In order to characterize this trend, the δ of the nine available days are binned by satellite elevation. The σ_δ values for each bin are plotted in Figure 4. This trend resembles the form of the ionosphere projection factor, called the Obliquity Factor (OF), which is further described in the subsequent section.

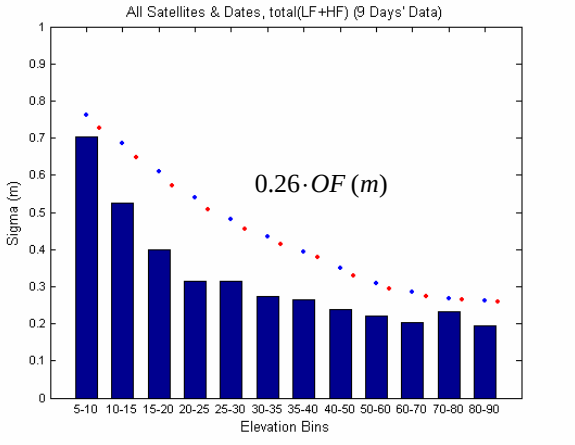

Figure 4. Simple Obliquity Factor Model for σ_δ

This observation supports Shively's earlier theoretical prediction that the WAAS error sigma (and hence the discrepancy statistic) might scale with obliquity factor [7]. Figure 4 plots the scaled obliquity factor model along with the discrepancy standard deviation. In order to provide an overbound for discrepancy sigma, the obliquity factor curve must be scaled by a factor of at least 0.26 meters.

The data described in this section provide experimental validation for availability simulations using the scaled OF model for discrepancy as a function of elevation. Before discrepancy data were available, for instance, the ranged-based LAM simulations of [1] computed availability for two hypothetical conditions, one assuming moderate levels of discrepancy (0.26·OF m) and the other assuming severe levels (0.39·OF m). The data in this section suggest that the availability computed for the moderate discrepancy model better reflect the actual availability of the LAM system.

TIME CORRELATION OF DISCREPANCY

This section demonstrates that the sigma model computed in the previous section, though appropriate for availability simulations, is not appropriate for continuity analysis, because of time correlation in the discrepancy signal.

A continuity break occurs if the discrepancy terms for one or more satellites fluctuate significantly after an aircraft begins an approach when those fluctuations cause VPL_{LAM} to exceed Vertical Alert Limit (VAL). The probability of a continuity break caused by a sudden jump in VPL_{LAM} is a strong function of time correlation in the discrepancy signal. Continuity analysis analyzes fluctuations in the VPL_{LAM} equation during the course of an approach (150 s). Because the correlation time for conventional LAAS is on the order of the duration of an approach, standard continuity analysis assumes that the error at the end of an approach is independent from the error at the beginning of the approach. In analyzing LAM, this assumption would treat the discrepancy statistic at the beginning and end of the approach as independent events, with a sigma described by the obliquity-factor model of the previous section.

This standard approach to continuity is extremely conservative for LAM, since the correlation time of the discrepancy statistic is an order of magnitude longer than the duration of an approach. There are apparently high and low frequency components in the discrepancy signal. The high frequency component is due to the discretization of the WAAS differential corrections and to receiver noise. The low frequency component is mainly related to troposphere modeling error. The troposphere effect is modeled in a coarse fashion by WAAS but is directly measured by LAM. Spectral analysis shows that the correlation time of the low frequency component of the discrepancy is 1000 seconds or more. This means that the

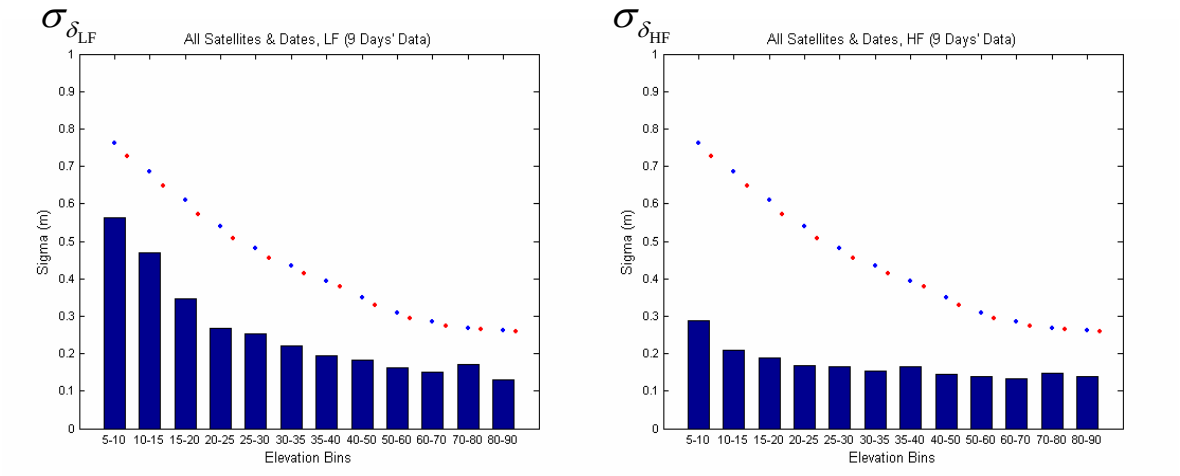

Figure 5. Different Elevation Dependencies of $\sigma_{\delta_{LF}}$, $\sigma_{\delta_{HF}}$

discrepancy varies little during a 150 second approach procedure.

The different characteristics of the low and high frequency components are clearly demonstrated in Figure 5. The low-frequency statistics are computed after first smoothing the data with a 2000-second moving-average filter. (The filter window length starts from 1 second when a satellite rises over the horizon and increases up to 2000 seconds) The high-frequency statistics are computed after differencing this smoothed, low-frequency discrepancy from the raw discrepancy signal.

As illustrated in figure 5, the low frequency component follows the trend of the OF model, in a manner similar to that seen for the raw divergence statistic in figure 4. By contrast, the high frequency component is almost flat over the entire elevation bins. The high $\sigma_{\delta_{HF}}$ at low elevation is partly due to the changing length of the filter window.

Future research will provide a precise assessment of the time correlation in the discrepancy signal through frequency-domain analysis. This analysis will enable a more accurate quantitative determination of LAM continuity.

PROTECTION LEVEL EVALUATION

In order to observe continuity and availability on a nominal day, it is useful to evaluate the Vertical Protection Level (VPL) using nominal days' data. An availability loss is indicated if the VPL_{H0} or VPL_{LAM} expressions exceed the Vertical Alert Limit (VAL) at any epoch. A continuity issue occurs if VPL_{LAM} exceeds VAL but VPL_{H0} does not. As an approximate model for a degraded constellation, it is useful to simply note that a potential continuity issue may occur whenever VPL_{LAM} exceeds VPL_{H0}.

In addition to providing a model useful for availability and continuity simulation, the available LAM data set also provides a means to validate LAM performance for a nominal day and, thereby, to enable selection of variable LAM parameters. System performance is computed by evaluating VPL as a function of time for each day's data. In a range-based LAM the fault-free error bound, VPL_{LAM}, is evaluated indirectly through manipulation of the user VPL_{H1} equation by a sigma mapping [1]. The user receiver's VPL_{H1} equation is replaced by VPL_{LAM} because the ground station maps the broadcast sigmas. In practice, LAM user receivers will also evaluate two legacy VPL expressions, both related to conventional LAAS: VPL_e and VPL_{H0}. These expressions have no role in LAM integrity, but they must be evaluated to maintain receiver compatibility between LAM and conventional LAAS.

The final value of VPL is the largest of all three expressions evaluated by the user, as shown in Figure 6. Of these three values, VPL_e is always the smallest, and, as a consequence, the expression may be neglected in VPL analysis. Experimental data can be used to examine the relationship between VPL_{LAM} and VPL_{H0} and, as a consequence, their impact on operating LAM performance. In order to evaluate these VPL expressions, it is first necessary to model the sigma parameters broadcast by a LAM ground station.

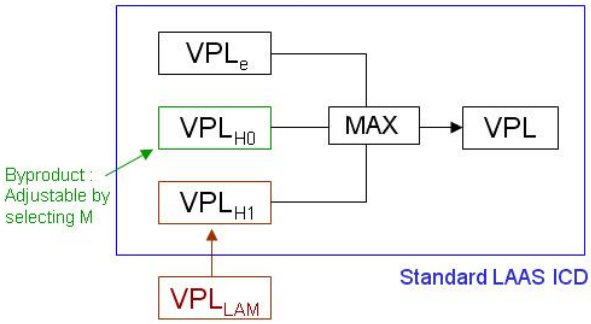

Figure 6. VPL Computation for a Range-Based LAM

Sigma Models

This section describes the sigma models used in evaluating VPL_{H0}, (5), and the deterministic term of VPL_{LAM}, (2). Furthermore, the detailed procedure to calculate the VPL_{LAM} is also described in this section.

Note that the tilde notation in (5) indicates that sigmas are mapped from their nominal values (in order to convert the standard VPL_{H1} equation into VPL_{LAM}). Detailed explanation about the sigma mapping and its compatibility with the standard LAAS Interface Control Document (ICD) is given in [1].

$$\mathrm{VPL}_{\mathrm{H0}} = K_{ffmd}\sqrt{\sum_{i=1}^{N} S_{v,i}^2 \tilde{\sigma}_{tot,i}^2} \qquad (5)$$

where $\tilde{\sigma}_{tot,i}^2 = \tilde{\sigma}_{gnd,i}^2 + \tilde{\sigma}_{air,i}^2 + \tilde{\sigma}_{iono,i}^2 + \tilde{\sigma}_{tropo,i}^2$

$$\tilde{\sigma}_{gnd,i}^2 = \frac{M_i - 1}{M_i}\left[\left(\frac{K_{bnd}}{K_{md}}\right)^2 \sigma_{L,i}^2 + \left(\left(\frac{K_{bnd}}{K_{md}}\right)^2 - 1\right)\sigma_{air,i}^2\right]$$

$$\tilde{\sigma}_{air,i} = \sigma_{air,i}$$

$$\tilde{\sigma}_{iono,i} = \frac{K_{bnd}}{K_{md}}\sigma_{iono,i}$$

$$\tilde{\sigma}_{tropo,i} = \frac{K_{bnd}}{K_{md}}\sigma_{tropo,i}$$

The geometry weighting factor, $S_{v,i}$ in VPL_{LAM} depends on the $\sigma_{tot,i}^2$ and satellite geometries. The $S_{v,i}$ is the third row of the S matrix for the i^{th} ranging source. The sensitivity (S) matrix is used for the weighted least squares estimate and the specific formula is given in the section 2.3.9 of the LAAS MOPS [6].

The LAM ground receiver error, $\sigma_{L,i}$ in (2) is modeled by the Ground Accuracy Designator (GAD) curve which is defined in the LAAS MASPS [5]. Specifically, the GAD-B1 curve is used here because the LAM ground station is assumed to employ a single choke-ring style antenna instead of a highly sophisticated Multipath Limiting Antenna (MLA) which is used for conventional LAAS. This consideration simplifies LAM complexity and lowers system cost compared to conventional LAAS.

The airborne error, $\sigma_{air,i}$, is assumed to be characterized by the Airborne Accuracy Designator B (AAD-B) curve which is also defined in [5].

Assuming a horizontal aircraft speed of 127 m/s, a separation between the aircraft and ground reference receiver of 6 km, and a vertical ionosphere gradient sigma (σ_{vig}) of 4 mm/km [8], the $\sigma_{iono,i}$ is obtained as follows [6].

$$\begin{aligned}\sigma_{iono,i} &= OF_i \times \sigma_{vig} \times (x_{air} + 2\tau v_{air}) \\ &= OF_i \times 0.004 \times (6 + 2 \times 100 \times 0.127)\ (m)\end{aligned} \qquad (6)$$

The obliquity factor, OF, is a unitless function of satellite elevation angle, defined in the LAAS MOPS [6].

$$OF_i = \left[1 - \left(\frac{R_e \cos\theta_i}{R_e + h_I}\right)^2\right]^{-\frac{1}{2}} \qquad (7)$$

The troposphere error, $\sigma_{tropo,i}$, is neglected because it has relatively small magnitude comparing to the other error sigmas.

The remaining parameter in the first term of (2), which has only deterministic components, is K_{bnd}. The VPL_{LAM} provides a confidence bound with a risk probability equal to the integrity allocation for fault-free operations. For the purpose of this data analysis, the integrity allocation for the fault-free VPL for the Category I operation is chosen as 2.5×10^{-8}, a value which was also used in [2]. The corresponding K_{bnd} is

$$K_{bnd} = Q^{-1}(2.5\times10^{-8}) = 5.451\,. \qquad (8)$$

Unlike the other parameters in the VPL_{LAM} equation, (2), the discrepancy for each satellite, δ_i is random variable evaluated through local monitoring. For the purpose of evaluating protection level, these random discrepancies

can be evaluated using the nine nominal days of field data available for Atlantic City. Discrepancy is computed using the position-domain bias removal method of equation (4).

Evaluating VPL_{LAM} and VPL_{H0} Using FAATC Data

This section applies the sigma models to compute VPL_{LAM} and VPL_{H0} for a typical user. Protection levels are evaluated through the entire data set of nine nominal days for the typical user employing all satellites in view.

A key parameter which controls the relative magnitude of VPL_{LAM} and VPL_{H0} is the number of B-values broadcast by the LAM ground station, M. This parameter effectively inflates VPL_{H0} through the ground sigma term, as described by (5). The inflation does not impact VPL_{LAM}, however.

Since the LAM broadcasts the same discrepancy values in each of the B-value channels, the LAM is free to broadcast between two and four B-values, as set by the LAAS Interface Control Document (ICD) [9]. By construction of the broadcast message, the margin between VPL_{H0} and VPL_{LAM} increases as the number of broadcast B-values increases. Figure 7 illustrates the continuity margin for a particular example: the case with two broadcast B-values (M = 2).

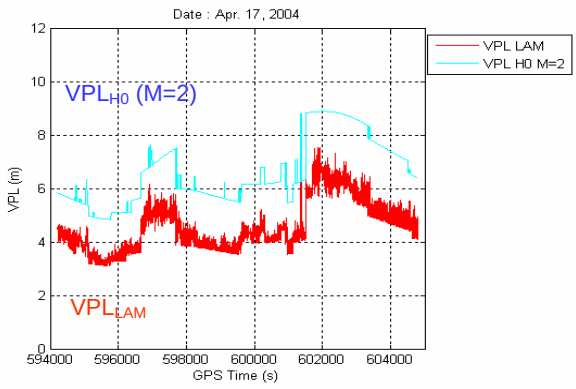

Figure 7. VPL_{LAM} and VPL_{H0} of an Entire Day (M=2)

As shown in Figure 7, VPL_{H0} is generally larger than VPL_{LAM} when the M parameter is set equal to two. Since the user always evaluates VPL as the larger of these two expressions, VPL_{H0} dominates over VPL_{LAM} under typical conditions. This result implies excess conservatism, since the smaller value of VPL_{LAM} is sufficient to ensure system integrity. Although the legacy VPL_{H0}, in effect, reduces system availability, this conservative VPL also plays an important role in ensuring system continuity, as described by [1].

A continuity break occurs when the aircraft observes VPL to jump suddenly above VAL during an approach operation. Because the VPL_{LAM} expression incorporates the discrepancy terms, δ_i, which are random variables, the VPL_{LAM} equation may result in a continuity break if the discrepancy terms increase abruptly. The larger magnitude of the VPL_{H0} equation provides continuity margin in case of such an event. A larger continuity margin reduces the risk than a δ spike causes VPL_{LAM} to exceed VPL_{H0} which implies a potential continuity issue.

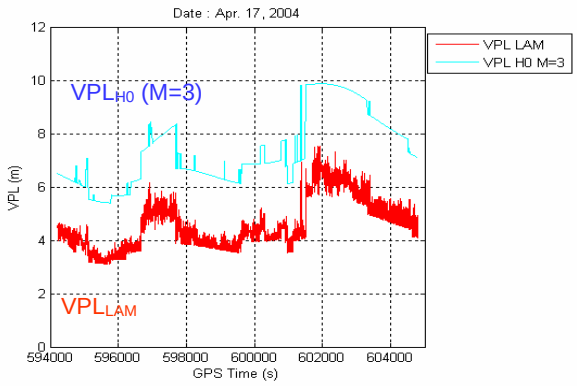

Figure 8. VPL_{LAM} and VPL_{H0} of an Entire Day (M=3)

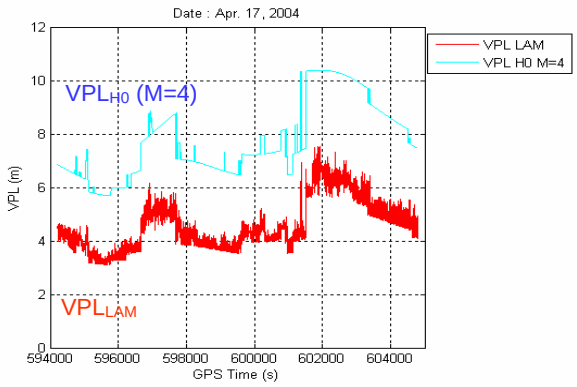

Figure 9. VPL_{LAM} and VPL_{H0} of an Entire Day (M=4)

Figures 7 through 9 illustrate the tradeoffs associated with the choice of M. A higher M introduces greater continuity margin at the expense of availability. LAAS receivers are capable of handling only three possible values of M: 2, 3, or 4.

For the case that M equals 4, as illustrated in Figure 9, the deterministic VPL_{H0} equation frequently exceeds 10 m. This will result in a substantial availability sacrifice under nominal conditions, unless VAL is increased from its standard value of 10 m to a value of 11 m (or greater). Although availability suffers for the M=4 case, continuity margin is high. For the case that M equals 2, as illustrated in Figure 7, VPL never exceeds 10 m, implying no availability penalty for operations under nominal

Table 1. Continuity Risk and Availability Loss

9 Nominal Days (273386 epochs)	$VPL_{LAM} > VPL_{H0}$ (epochs)	Protected Continuity Risk (%)	VAL (m)	VPL_{LAM} or VPL_{H0} > VAL (epochs)	Availability (%)
M = 2	118	99.9568	10	494	99.8193
			12	301	99.8899
M = 3	32	99.9883	10	4509	98.3517
			12	301	99.8899
M = 4	19	99.9931	10	8789	96.7851
			12	494	99.8193

conditions. Continuity margin is low for the M=2 case, but, at least in the day depicted by the figure, there is no VPL_{LAM} spike which exceeds VPL_{H0}. Figure 8 indicates that a compromise is achieved for the M=3 case. In this case, the nominal user achieves full availability through the day, with VPL always below 10 m. This matches the nominal availability for the M=2 case, while significant improving continuity margin.

Table 1 summarizes availability and continuity risk observed in the entire data set. If the VAL for LAM is set to its standard value of 10 m, best performance is achieved by setting M to 2. Although the continuity risk is highest for the M=2 case, it is the only one of the allowed values of M that achieves an availability above 99% for a 10 m VAL. If VAL were increased to a 12 m level, best performance would be achieved by setting M to 4. In the case of a 12 m VAL, all three settings achieve nearly identical availability. The M=4 case, however, minimizes continuity risk.

Observed Anomalous Behavior

Instances of availability loss and continuity risk result from different underlying phenomena. Availability loss, when VPL_{LAM} or $VPL_{H0} > VAL$, is mainly caused by bad satellite geometries which increase VPL_{H0} and the deterministic term of VPL_{LAM}. On the other hand, instances of the possible continuity loss, when $VPL_{LAM} > VPL_{H0}$, are due to sudden spikes in discrepancy. Discrepancy spikes increase the discrepancy term of VPL_{LAM}, $\left|\sum_{i=1}^{N} S_{v,i}\delta_i\right|$, and, in some cases, cause VPL_{LAM} to exceed VPL_{H0}. These two cases are well observed in May 16, 2004 data in Figure 10.

An availability loss occurred, for example, on May 16 at a time of 75900 s, when VPL rapidly increased above VAL. The VPL increase occurred when the number of visible satellites dropped briefly from seven to six, as illustrated in Figure 11. Because the LAM approves satellites only when both a WAAS correction and a local measurement are available, instances of bad geometry may occur if a WAAS correction is not available or if the LAM receiver fails to track a low-elevation satellite that might otherwise be in view.

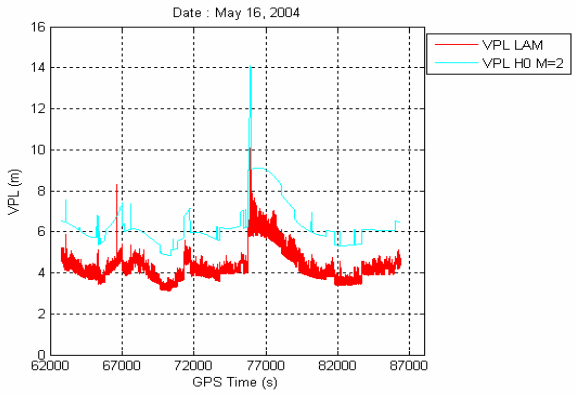

Figure 10. Availability Loss and Continuity Risk

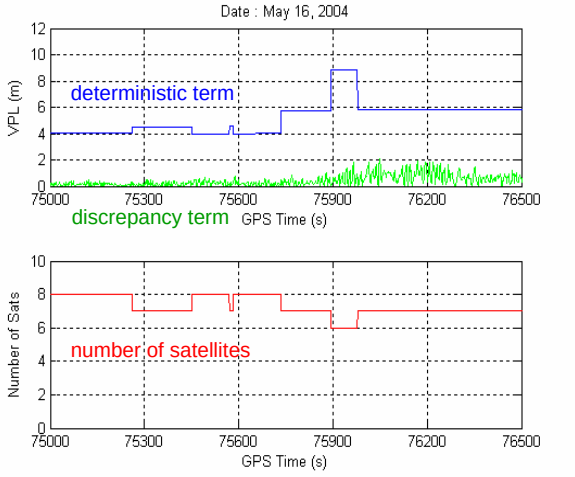

Figure 11. VPL Spikes due to Bad Geometries

On May 16, an instance of potential continuity risk, with $VPL_{LAM} > VPL_{H0}$, occurred at 66600 s. The WAAS correction for PRN 10 does not immediately follow the sudden change in LAAS correction in Figure 12. This time delay causes a discrepancy spike for PRN 10 and the spike propagates to the discrepancy term of VPL_{LAM}, $\left|\sum_{i=1}^{N} S_{v,i}\delta_i\right|$, and finally to the VPL_{LAM} itself. These events with VPL_{LAM} greater than VPL_{H0} are rare, especially if M is set equal to 4. For the available data with M=4, this event occurs only during one 32 second interval, during which VPL_{LAM} fluctuates and exceeds VPL_{H0} for a total of 19 seconds.

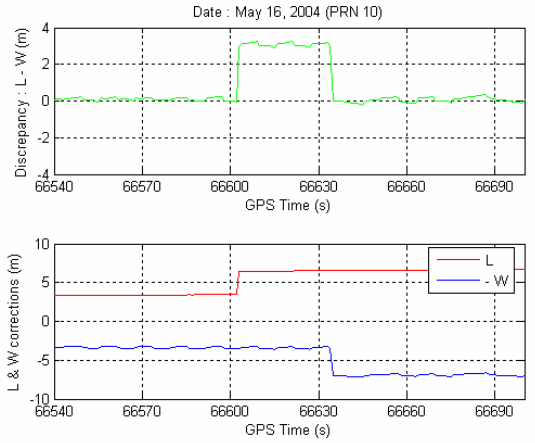

Figure 12. Discrepancy Spike and Time Delay between LAAS and WAAS corrections

VARIATION OF DISCREPANCY BIASES

In analyzing the random component of the discrepancy statistic a position-domain bias term was removed, according to (4). This bias term was computed using a day-long average, and thus would not be removed from the discrepancy broadcast in real time, computed using (1). If this position-domain bias were small, it would have little impact on LAM performance. As discussed in this section, however, the position-domain bias may be as large as half a meter, or more. Biases of this size would have a significant impact on both system availability and continuity.

Though the individual ranging signals were unbiased, the resulting position-domain solution of the measured discrepancy signal contained an offset that persisted throughout each day-long data set. This section describes the impacts of the position-domain bias on system performance parameters including integrity, availability, and continuity.

Frame Correction and Residual Bias

The analyses in the previous sections are based on a discrepancy, δ which is free from position-domain bias by (4). If the bias were not removed from the data, the impact would result in increased VPL_{LAM} as illustrated in Figure 13 and 14. The bias would increase the second term of VPL_{LAM} equation, $\left|\sum_{i=1}^{N} S_{v,i}\delta_i\right|$, which contains the discrepancy term, δ_i, and accordingly increase VPL_{LAM}. The increased VPL_{LAM} negatively impacts system availability and continuity. System integrity is not affected, since any biases in the discrepancy statistic directly enter the VPL_{LAM} equation.

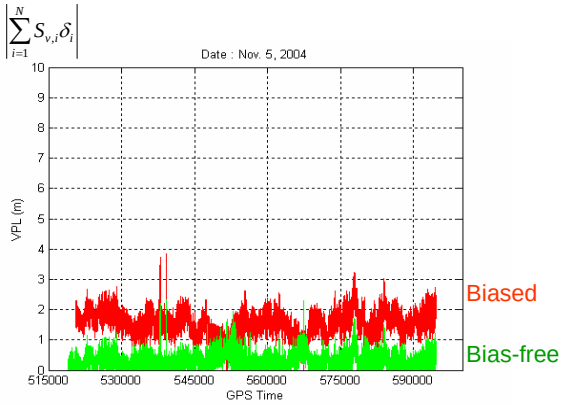

Figure 13. Impact of Position-Domain Bias on the Second Term of VPL_{LAM}

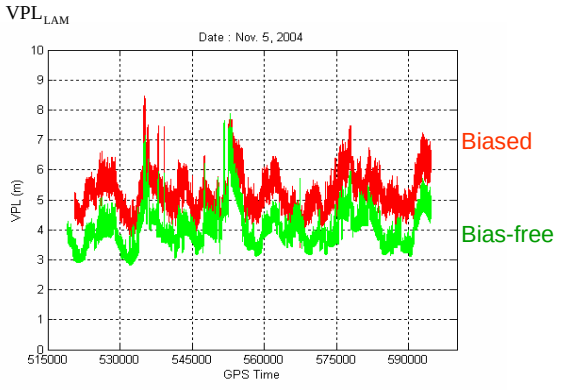

Figure 14. Impact of Position-Domain Bias on VPL_{LAM}

The position-domain bias affects not only the vertical error, but the lateral navigation error as well. Figure 15 clearly shows strong biases in the vertical, East and North directions. The bias is highest in the vertical direction, at approximately 1.5 m. The mathematical expressions of the vertical, east, and north components of projection are $\sum_{i=1}^{N} S_{v,i}\delta_i$, $\sum_{i=1}^{N} S_{e,i}\delta_i$, and $\sum_{i=1}^{N} S_{n,i}\delta_i$ respectively.

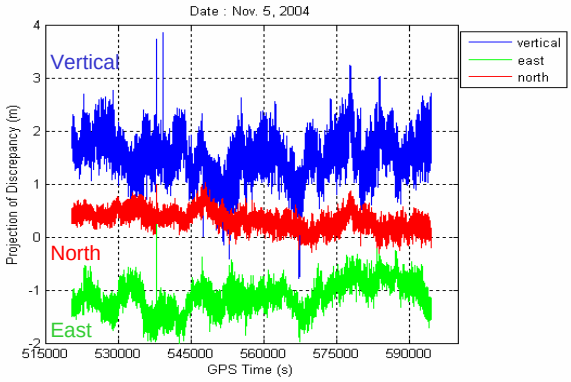

Figure 15. Position-Domain Projection of the δ

The position-domain bias in the Atlantic City data can be explained, in large part, by the difference between the reference frames used by LAAS and WAAS. The LAAS reference frame is the North American Datum of 1983 (NAD83), and the WAAS reference frame is the International Terrestrial Reference Frame (ITRF). In order to remove this reference frame difference, it is necessary that the LAM convert the broadcast WAAS corrections and the broadcast final-approach segment data into a common reference frame.

After the NAD83 to ITRF reference frame correction which was performed by FAATC using a closed form frame transformation equation, the residual biases in Figure 15 were decreased to a level of only 10 to 20 cm for the November 5, 2004 data set. The improvement is illustrated in Figure 16.

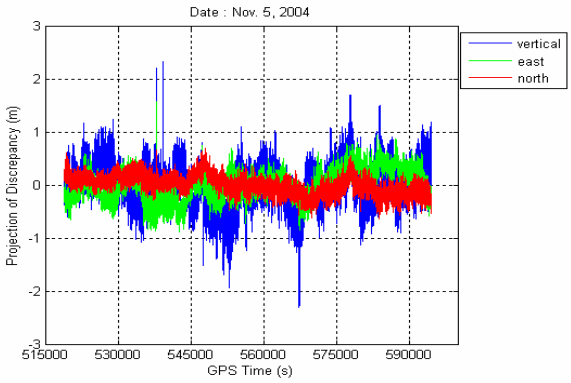

Figure 16. Position Domain Projection of the δ after Frame Correction

Although residual biases after frame correction were small for the reference day of November 5, 2004, residual biases were significantly larger for other days of data. These differences in bias level cannot be explained by the small changes in the reference-frame calibration that results from continental drift.

Long-term Variation of Residual Bias

The residual position-domain bias varied significantly between each day-long data set over the year of 2004, as illustrated in Figure 17.

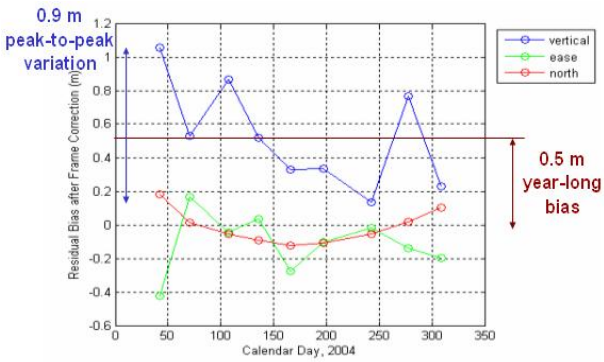

Figure 17. Variation of Residual Bias over a Year

The vertical residual biases were all positive, implying a probable antenna calibration bias in the vertical direction of 0.5 m. If the 0.5 m long-duration bias were removed, there would still be ± 0.45 m spread in data Reference frame drift over a year is less than 10 cm, so the ± 0.45 m spread is too large to account for considering continental drift alone. A likely cause for the discrepancy is a long-duration, widespread discrepancy in the troposphere away from the standard model used by WAAS.

These residual position-domain biases will have a significant impact on the availability and continuity of the LAM system. Integrity is still protected, however, because the VPL_{LAM} equation automatically computes the total discrepancy for all satellites in the position-domain.

In LAM availability analysis, the discrepancy signal must be modeled to include the bias term. This modification will result in larger simulated VPL_{LAM} and a lower availability. The continuity effect is a loss of some of the margin provided by VPL_{H0}. If these effects are too severe, LAM may be required to estimate position-domain bias on the fly.

CONCLUSION

There are four important results which have been uncovered by the analysis of LAM field data performed in this paper. These results impact the continuity and availability analysis of LAM.

First, the discrepancy sigma model which has been used for previous availability simulation is validated based on experimental data. The discrepancy sigma, σ_δ , is strongly dependent on elevation but not on WAAS UDRE.

Second, time-correlation in the discrepancy statistic, δ , is large and should be considered for precise continuity analysis. A new frequency-based approach for LAM continuity assessment is recommended as a topic for future research.

The number of broadcast B-values, M, is a parameter that controls VPL_{H0} level and, accordingly, continuity margin. If the VAL for LAM is set to 10 m, best performance is achieved for M equal 2. Based on VPL evaluation of the entire data set with VAL equal 10 m, the M=2 case achieves better than 99.8% availability and protects continuity risk for 99.9% of epochs. If the VAL for LAM is set to 12 m or higher, best performance is achieved for M equal 4. Based on VPL evaluation of the entire data set with VAL equal 12 m, the M=4 case protects the continuity risk for 99.99% of epochs while achieving 99.8% availability.

Finally, it is revealed that long-duration position-domain biases are present in field data. These position-domain biases fluctuate significantly among each of the nine day-long data sets analyzed in this paper. These fluctuations, which may result from discrepancy between the actual troposphere and the WAAS troposphere model, do not impact LAM integrity, but may reduce availability and continuity below levels described in previous research .

ACKNOWLEDGMENTS

The authors gratefully acknowledge the Federal Aviation Administration Satellite Navigation LAAS Program Office (AND-710) for supporting this research. The opinions discussed here are those of the authors and do not necessarily represent those of the FAA or other affiliated agencies.

REFERENCES

[1] J. Rife, S. Pullen, T. Walter and P. Enge, *Vertical Protection Levels for a Local Airport Monitor for WAAS*, Proceedings of the Institute of Navigation's ION-AM 2005.

[2] C.A. Shively, R. Niles, T.T. Hsiao, *Performance and Availability Analysis of a Simple Local Airport Position Domain Monitor for WAAS*, Proceedings of the Institute of Navigation's ION-GNSS 2005.

[3] T. Walter, S. Pullen, J. Rife, J. Seo, and P. Enge, *The Advantages of Local Monitoring and VHF Data Broadcast for SBAS*, Proceedings of the European Navigation Conference GNSS 2005, Munich, Germany.

[4] RTCA Inc, *Minimum Operational Performance Standards for GPS/Wide Area Augmentation System Airborne Equipment*, RTCA/DO-229C, November 28, 2001.

[5] RTCA Inc, *Minimum Aviation System Performance Standards for the Local Area Augmentation System (LAAS)*, RTCA/DO-245, 1998.

[6] RTCA Inc, *Minimum Operational Performance Standards for GPS Local Area Airborne Equipment*, RTCA/DO-253A, November 28, 2001.

[7] C. Shively and T. Hsiao, *WAAS Airport Position Monitor Concept and Feasibility Requirements (Preliminary)*, FAA LAM Telecon, February 15, 2005.

[8] C. Shively and T. Hsiao, *Availability Enhancements for CAT IIIB LAAS*, NAVIGATION, Journal of the Institute of Navigation, Vol. 51, No. 1, Spring 2004.

[9] RTCA Inc, *GNSS-Based Precision Approach Local Area Augmentation System (LAAS) Signal-in-Space Interface Control Document (ICD)*, RTCA/DO-246B, November 28, 2001